Effects of Spatial Dispersion on Reflection From Mushroom-Type Artificial Impedance Surfaces

Olli Luukkonen, Mário G. Silveirinha, *Member, IEEE*, Alexander B. Yakovlev, *Senior Member, IEEE*, Constantin R. Simovski, *Member, IEEE*, Igor S. Nefedov, *Member, IEEE*, and Sergei A. Tretyakov, *Fellow, IEEE*

***Abstract*—In a spatially dispersive medium, the electric dipole moment of an inclusion cannot be related to the macroscopic electric field through a local relation. Several recent works have emphasized the role of spatial dispersion in wire media, and demonstrated that arrays of parallel metallic wires may behave very differently from a uniaxial local material with negative permittivity. Here, we investigate the effect of spatial dispersion on reflection properties of the mushroom structure introduced by Sievenpiper, based on local and nonlocal homogenization methods. The objective of this paper is to clarify the role of spatial dispersion in the mushroom structure and demonstrate that, under some conditions, it is suppressed. The metamaterial substrate, or metasurface is modeled as a wire medium covered with an impedance surface. Surprisingly, it is found that, in such a configuration, the effects of spatial dispersion may be nearly suppressed when the slab is electrically thin, and that the wire medium can be modeled very accurately using a local model.**

***Index Terms*—Analytical modeling, high-impedance surfaces, mushroom structures, reflection properties, spatial dispersion, wire medium.**

I. Introduction

ARTIFICIAL impedance surfaces such as the corrugated surfaces (see, e.g., [1]) have been studied for decades. However, it was only after the seminal paper of Sievenpiper *et al.* [2] that the interest toward the artificial or *high-impedance* surfaces increased significantly in the literature. The exotic features and engineerable response of these surfaces have resulted in many novel and improved applications such as quasi-TEM [3] and impedance waveguides [4], [5], bandgap structures [6], low-profile antennas [7], [8], leaky-wave antennas [9], [10], and absorbers [11]–[14], just to name a few.

In parallel with the research of new possibilities to exploit the features of these exotic surfaces, attempts to fully understand the physics behind the surface behavior have also been conducted. This research has resulted in analytical formulas for different artificial impedance surfaces providing physical insight and engineering tools for the designers. In some cases, the analyses are based on the Floquet expansion of the scattered field [15], [16], whereas some models use extraction methods to fit the model for surfaces. In other models, the complete artificial impedance surface structure is treated as a grounded slab of a material with given permittivity and permeability tensors [17]. Although these models would predict the response of the surfaces accurately, they are either complicated or lack real physical basis.

In our previous study [18], surfaces formed by an array of rectangular patches over a grounded dielectric slab were considered, and an accurate spatially dispersive (SD) model for the patch array was derived. This model for the patch array was later used in the presence of a grounded dielectric slab perforated with metallic vias [5]. The perforated dielectric substrate was modeled in the case of electrically thin substrates as a uniaxial material with local negative permittivity. The corresponding artificial dielectric, designated here as wire medium, is reasonably well known in the microwave engineering [19], [20], where the wire medium was initially proposed to simulate electron plasma. However, the wire medium has recently become known to exhibit spatial dispersion [21]. Nonlocal properties of the wire medium have been used favorably, for instance, in subwavelength imaging [22]–[24] or artificial impedance surfaces [25]–[27].

In [25]–[27], the grounded wire medium slab or "Fakir's bed of nails" has been studied taking the SD characteristics of the wire medium into account. These works have demonstrated that the wire medium may behave very differently from a uniaxial material with local negative permittivity. It was proven that in the limit $a/h \to 0$ (h is the length of the wires and a is the lattice constant), the structured material behaves instead as a material with extreme anisotropy with the relative permittivity along the wires approaching to infinity and the relative transverse permittivity equaling unity. Based on these results, it is natural to ask if spatial dispersion may also play an important role in the mushroom structure since it can be regarded as a wire medium capped with a frequency-selective surface (FSS), as was done e.g., in [5], [17], and [28]. In these studies, it was shown that the response of the mushroom-type artificial impedance surface may be predicted accurately by considering that the wire medium behaves as a uniaxial material with local negative permittivity, in apparent contradiction with the studies of [21], [25], and [27].

To study these issues, here we derive a homogenization model for the mushroom structure that fully takes into account the effects of spatial dispersion in the wire medium. Our objective

Manuscript received October 12, 2008. First published October 09, 2009; current version published November 11, 2009. This work was supported in part by the Academy of Finland under the Center-of-Excellence Program.

O. Luukkonen, C. R. Simovski, I. S. Nefedov, and S. A. Tretyakov are with the Department of Radio Science and Engineering/SMARAD CoE, TKK Helsinki University of Technology, FI-02015 TKK, Finland (e-mail: olli.luukkonen@tkk.fi).

M. G. Silveirinha is with the Departmento de Engenharia Electrotécnica, Instituto de Telecomunicações, Universidade de Coimbra, 3030 Coimbra, Portugal.

A. B. Yakovlev is with the Department of Electrical Engineering, The University of Mississippi, University, MS 38677-1848 USA.

Color versions of one or more of the figures in this paper are available online at http://ieeexplore.ieee.org.

Digital Object Identifier 10.1109/TMTT.2009.2032458

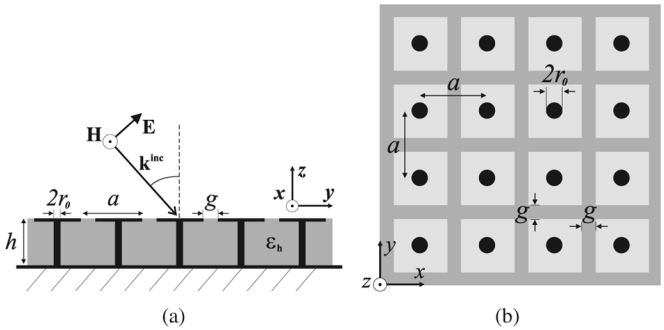

Fig. 1. Illustration of the mushroom structure. (a) From the side. (b) From above. The structure comprises a patch array over a dielectric slab perforated with metallic vias. The periodicity of the vias and patches is a, the gap between the adjacent patches g, the radius of the vias r_0, and the relative permittivity of the host medium ε_h.

in this paper is to clarify the role of spatial dispersion in the mushroom structure due to the discrepancies mentioned above in the treatment of the wire medium. Surprisingly, our results show that unlike in the topology for which the array of patches is removed (i.e., in the "Fakir's bed of nails" studied in [25]), the effect of spatial dispersion may be nearly negligible in the mushroom structure when the wire medium slab is electrically thin [29]–[32]. This result is in good agreement with the results of [33], where it was also noticed that by connecting conductive structures, such as metal plates, to the wires, the spatial dispersion in wire medium can be avoided. In such circumstances, the wire medium may be modeled to a good approximation as a uniaxial material with local negative permittivity. We demonstrate that the effects of spatial dispersion are significant in mushroom structures only for rather thick wire medium slabs and at high frequencies.

The rest of this paper is organized as follows. First, we will discuss and derive two analytical models of the electromagnetic response of the mushroom structure. One of the models takes into account the effect of spatial dispersion in the wire medium, while the other model assumes that the wire medium has a local response. Based on the homogenization results, we will discuss in which circumstances the spatial dispersion effects are suppressed. In Section III, we will then validate the two models against full-wave simulations, demonstrating that by taking into account spatial dispersion, we obtain an accurate model for the response of the mushroom structures. However, under some circumstances, which are well applicable to most of the practical high-impedance surfaces, the simple model neglecting the spatial dispersion in the wire medium is accurate and perfectly capable of predicting the response of the surface to incident plane waves.

II. Analytical Models for the Mushroom Structure

A schematic picture of the mushroom structure comprising an array of patches over a dielectric layer perforated with metallic vias is shown in Fig. 1. It should be noted that the models proposed in this study are also applicable for other topologies of the mushroom structure, as will be discussed later. Here, the patch array serves merely as a good example for its SD electromagnetic properties have been studied in our previous work [18]. The surface impedance describing the electromagnetic properties of the square patch array reads [18]

$$Z_g^{\mathrm{TM}} = -j\frac{\eta_{\mathrm{eff}}}{2\alpha} \tag{1}$$

with $\eta_{\mathrm{eff}} = \sqrt{\mu_0/\varepsilon_0\varepsilon_{\mathrm{eff}}}$, and the grid parameter α is given by

$$\alpha = \frac{k_{\mathrm{eff}}a}{\pi}\ln\left(\sin^{-1}\left(\frac{\pi g}{2a}\right)\right) \tag{2}$$

where $k_{\mathrm{eff}} = k_0\sqrt{\varepsilon_{\mathrm{eff}}}$, a is the period of the array, g is the gap between the adjacent patches, and k_0 is the wavenumber in free space. Furthermore, the effective relative permittivity reads

$$\varepsilon_{\mathrm{eff}} = \frac{\varepsilon_h + 1}{2} \tag{3}$$

where ε_h is the relative permittivity of the supporting host medium.

We model the dielectric slab perforated with metallic vias as wire medium, which can be described with an effective relative permittivity tensor having values only along its diagonal. The dyadic permittivity for the case depicted in Fig. 1 reads $\overline{\overline{\varepsilon}}_{r,\mathrm{eff}} = \varepsilon_h\left(\hat{\mathbf{u}}_x\hat{\mathbf{u}}_x + \hat{\mathbf{u}}_y\hat{\mathbf{u}}_y\right) + \varepsilon_{zz}\hat{\mathbf{u}}_z\hat{\mathbf{u}}_z$, where ε_h is the relative permittivity of host medium and ε_{zz} is the effective relative permittivity along the vias. In what follows, we describe two analytical models for the electromagnetic response of the considered structured substrate. The main difference between the two models is related to how the wire medium slab is treated. The second model, described in Section II-B, considers only the effects of frequency dispersion in the wire medium, and assumes that the material has a local response. However, it is known that the wire medium suffers from spatial dispersion even at very low frequencies [21]. It is also known that for an electrically thin wire medium slab (with no patch array) the charges accumulate on the tips of the metallic vias and the effects of spatial dispersion need to be taken into account [25]. For this reason, in Section II-A, we describe a nonlocal model that takes both TM- (with respect to the z-direction) and TEM-polarized waves into account in the wire medium slab. In this case, we assume that the effective relative permittivity of the wire medium slab along the vias has both frequency and spatial dispersion.

A. Nonlocal Model for the Wire Medium

For long wavelengths, the relative effective permittivity of the wire medium along the metallic vias (normal direction) can be written for the nonlocal model as [21]

$$\varepsilon_{zz} = \varepsilon_h\left(1 - \frac{k_p^2}{k^2 - q_z^2}\right) \tag{4}$$

where $k = k_0\sqrt{\varepsilon_h}$ is the wavenumber in the host medium, q_z is the z-component of the wave vector $\mathbf{q} = (q_x, q_y, q_z)$, and k_p is the plasma wavenumber for square lattices given as [21]

$$(k_p a)^2 = \frac{2\pi}{\ln\left(\dfrac{a}{2\pi r_0}\right) + 0.5275} \tag{5}$$

with a being the period of the vias (the same period with the patch array) and r_0 is the radius of the vias (see Fig. 1).

A TM-polarized incident plane wave excites TEM- and TM-polarized plane waves in the wire medium slab through the capacitive array. For these two plane waves, we have the following dispersion equations:

$$k = \pm q_z \quad \text{(TEM mode)} \tag{6}$$

$$k^2 = k_p^2 + \mathbf{q}\cdot\mathbf{q} \quad \text{(TM mode)}. \tag{7}$$

In [25], [26], the grounded wire medium slabs were characterized by solving the field amplitudes in all space. Omitting the dependence on the y-coordinate ($e^{-jk_y y}$), we can write the field amplitudes for the magnetic fields similarly as

$$H_x = \begin{cases} e^{jk_z z} + \rho e^{-jk_z z}, & \text{if } z > 0 \\ A_{\mathrm{TEM}}\cos\left(k(z+h)\right) + A_{\mathrm{TM}}\cosh\left(\gamma_{\mathrm{TM}}(z+h)\right), \\ \quad \text{if } -h < z < 0 \end{cases} \tag{8}$$

where $k_z = \sqrt{k_0^2 - k_t^2}$, $\gamma_{\mathrm{TM}} = \sqrt{k_p^2 + k_t^2 - k^2}$, and k_t is the transverse wavenumber, which is determined by the angle of incidence. In order to solve for the unknowns ρ, A_{TEM}, and A_{TM}, an additional boundary condition (ABC) is needed. In [27], an ABC was derived for the interface between air and the wire medium. This ABC is not applicable in the present problem because the patch array is connected to the wires. However, in [26], an ABC that properly models the connection between the wire medium and a metallic surface was derived, and such an ABC is also applicable in our case. It should be noticed that this boundary condition assumes that the charge density vanishes at the connection point of the metallic wire and the element of the capacitive array. This condition does not always hold; for instance, in cases where the array element size is of the same order as the diameter of the wire. Anyway, for high-impedance surfaces, such as the mushroom structure studied here, this is seldom the case because miniaturization of the surfaces leads inevitably to increased effective capacitance of the high-impedance surface. This, in turn, leads to a small gap size between the adjacent patches and to a large array element size (with respect to the period of the array).

In our case, the ABC reads on the wire medium side of the patch array ($z = 0^-$) as [26]

$$\frac{d}{dz}\left(\omega\varepsilon_0\varepsilon_h\hat{\mathbf{u}}_z\cdot\mathbf{E} + (\hat{\mathbf{u}}_z\times\mathbf{k_t})\cdot\mathbf{H}\right) = 0$$

$$\Rightarrow k_0\varepsilon_h\frac{dE_z}{dz} - k_t\eta_0\frac{dH_x}{dz} = 0. \tag{9}$$

As in [27], the remaining boundary conditions are obtained from the classical boundary conditions with the exception that, in our case, the transverse magnetic field is discontinuous over the patch array. Thus, at the interface between the wire medium and air ($z = 0$), we have the following conditions of continuous tangential electric field and discontinuous tangential magnetic field, respectively:

$$E_y|_{z=0^+} - E_y|_{z=0^-} = 0 \tag{10}$$

$$H_x|_{z=0^+} - H_x|_{z=0^-} = Z_g^{-1}E_y. \tag{11}$$

Here, Z_g is the surface impedance of the patch array given by (1). In (9)–(11), the values for the z- and y-components of the electric field are calculated from (8) by using Maxwell's equations, taking into account that the material has a nonlocal response and that the permittivity tensor depends on the considered mode.

Finally, using (9)–(11), we can solve the reflection coefficient ρ (for the magnetic field) from (8) unambiguously as follows:

$$\rho = \frac{\frac{\varepsilon_{zz}^{\mathrm{TM}}}{\gamma_{\mathrm{TM}}}\coth\left(\gamma_{\mathrm{TM}}h\right) + \frac{\varepsilon_{zz}^{\mathrm{TM}}-\varepsilon_h}{k}\cot\left(kh\right) + \frac{\eta_0}{jk_0}Z_g^{-1} - \frac{1}{jk_z}}{\frac{\varepsilon_{zz}^{\mathrm{TM}}}{\gamma_{\mathrm{TM}}}\coth\left(\gamma_{\mathrm{TM}}h\right) + \frac{\varepsilon_{zz}^{\mathrm{TM}}-\varepsilon_h}{k}\cot\left(kh\right) + \frac{\eta_0}{jk_0}Z_g^{-1} + \frac{1}{jk_z}} \tag{12}$$

where the relative effective permittivity along the direction of the metallic vias is written for the TM polarization using (4) and (7) as

$$\varepsilon_{zz}^{\mathrm{TM}} = \varepsilon_h\left(1 - \frac{k_p^2}{k_p^2 + k_t^2}\right). \tag{13}$$

The reflection coefficient ρ given in (12) can be used to characterize the electromagnetic properties of the high-impedance surface in the case of TM-polarized plane wave excitation. For a TE-polarized incident wave, the transverse electric field does not excite the metallic vias. In this case, the models presented in [18] can be applied for modeling the response of the surface. Furthermore, the present model is not only applicable for this particular type of high-impedance surface structure, but for other type of surfaces as well, as long as the structure consists of a wire medium slab. In these cases, Z_g, responsible for the interaction with the capacitive array, should be recalculated appropriately.

Using (9)–(12), we can also solve (8) for the amplitudes of the magnetic fields inside the high-impedance surface structure. We use them to determine the microscopic current on the metallic wires and use this quantity in order to validate our assumptions on the current phase variation in the case of the local model for the wire medium, as will be discussed ahead. The averaged current along the metallic wires can be written in terms of averaged macroscopic fields and the microscopic current I as (see [26])

$$J_{av,z} = \frac{1}{a^2}I = -j\omega\varepsilon_0\varepsilon_h E_z + jk_t H_x. \tag{14}$$

B. Local Model for the Wire Medium

In this model, for the high-impedance surface, we assume that the effective relative permittivity of the wire medium slab along the direction of the metallic vias can be described using the local model

$$\varepsilon_{zz}^{\mathrm{loc}} = \varepsilon_h\left(1 - \frac{k_p^2}{k_0^2\varepsilon_h}\right). \tag{15}$$

In this approximation, we have assumed the current phase variation along the wires to be small and the patch array over the wire medium slab to operate as a nearly perfect reflector. Due to the two mirror boundaries, the wires appear infinitely long for the electromagnetic wave inside the grounded wire medium slab. In addition, the small current phase variation along the vias

suggests that the waves can propagate mainly along the transverse direction inside the wire medium ($q_z \approx 0$), which makes, together with the infinite vias, our quasi-static approximation justified. Within this model, the incident plane wave excites a single mode (the extraordinary wave) inside the wire medium. It should be emphasized that, in general, the properties of this extraordinary mode have nothing to do with the properties of either the TEM or TM waves predicted by the nonlocal model. This model that treats the wire medium slab using the local approximation for the effective permittivity will be referred to as epsilon-negative (ENG) model from here on in order to distinguish it from the model derived in the previous section. As discussed in the previous section, that model uses the nonlocal (SD) approximation for the effective permittivity and requires the use of ABCs. For this reason, the model presented in Section II-A is referred to as the SD model hereafter.

A simple, yet accurate analytical model for the mushroom structure using this local approximation of permittivity of the wire medium slab has been derived in our previous work [5]. In order to compare the results of this paper with our previous results, we rewrite the results of [5] in a form similar to (12). After some algebra, the results of [5] can be rewritten for the magnetic field reflection coefficient in the following form:

$$\rho_{\rm loc} = \frac{\dfrac{\varepsilon_h}{\gamma_{\rm loc}}\coth\left(\gamma_{\rm loc}h\right) + \dfrac{\eta_0}{jk_0}Z_g^{-1} - \dfrac{1}{jk_z}}{\dfrac{\varepsilon_h}{\gamma_{\rm loc}}\coth\left(\gamma_{\rm loc}h\right) + \dfrac{\eta_0}{jk_0}Z_g^{-1} + \dfrac{1}{jk_z}} \tag{16}$$

where the propagation constant along the z-axis in the local approximation is given as

$$\gamma_{\rm loc} = \sqrt{\frac{k_t^2}{\varepsilon_{zz}^{\rm loc}} - k_0^2\varepsilon_h}. \tag{17}$$

When comparing the SD model with the ENG model, i.e., (12) and (16), we find that the difference between the two models lies on how they treat the surface impedance of the grounded wire medium slab, as stated earlier in this paper. For the SD and ENG models, the normalized surface admittances read, respectively, as

$$y_{s,\rm SD} = \frac{\varepsilon_{zz}^{\rm TM}}{\gamma_{\rm TM}}\coth\left(\gamma_{\rm TM}h\right) + \frac{\varepsilon_{zz}^{\rm TM}-\varepsilon_h}{k}\cot\left(kh\right) \tag{18}$$

$$y_{s,\rm ENG} = \frac{\varepsilon_h}{\gamma_{\rm loc}}\coth\left(\gamma_{\rm loc}h\right). \tag{19}$$

The surface admittance is given in terms of the normalized surface admittance as $Y_s = jy_sk_0/\eta_0$.

III. Numerical Validation

In order to compare the model derived in this paper, (12), and the result of our previous study (16), we use these models to characterize two particular high-impedance surfaces. We will do the characterization in terms of reflection phase diagrams for the electric field. We will also validate the results by numerical simulations obtained with Ansoft's High Frequency Structure Simulator (HFSS)[1] and with CST Microwave Studio.[2] Following the notations in Fig. 1, the parameters for the two cases read as follows ($r_0 = 0.05$ mm in both cases).

- $a = 2$ mm, $g = 0.2$ mm, $h = 1$ mm, and $\varepsilon_h = 10.2$.
- $a = 1$ mm, $g = 0.1$ mm, $h = 5$ mm, and $\varepsilon_h = 1$.

The reflection phases according to the SD and ENG models are given in Fig. 2(a) and (b), respectively. Quite interestingly, the general agreement between the two models for this example is excellent, notwithstanding the fact that each model describes the wire medium slab with very different material parameters. It is also seen that both models agree very well with the HFSS results. In the absence of losses, the ENG model shows some spurious resonances on a very narrow frequency band in the close vicinity of the plasma frequency of the wire medium

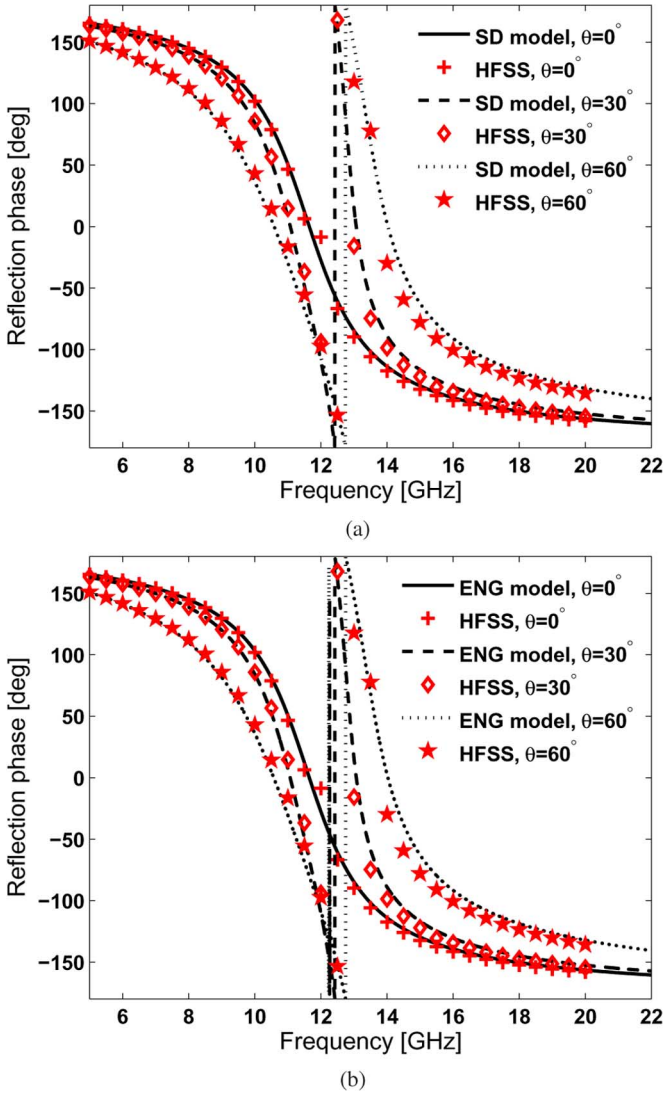

Fig. 2. Reflection phase calculated using: (a) SD model in (12) and (b) ENG model in (16) for the first example: $a = 2$ mm, $g = 0.2$ mm, $h = 1$ mm, $\varepsilon_r = 10.2$, and $r_0 = 0.05$ mm.

[1]Ansoft's homepage. [Online]. Available: http://www.ansoft.com/

[2]CST's homepage. [Online]. Available: http://www.cst.com/

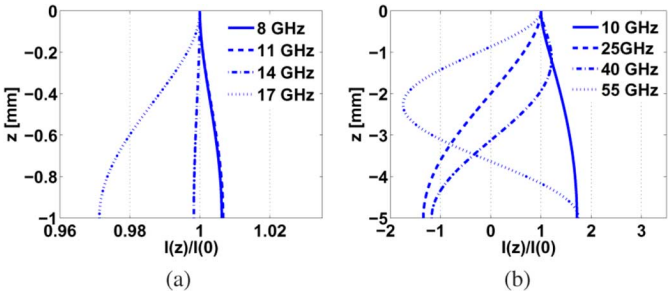

Fig. 3. Current magnitudes at different frequencies: (a) for the first example structure and (b) for the second example structure normalized to the current value on the patch array ($h = 0$). The reader should notice the different frequencies and scales in the plots. The angle of incidence is 30° for all cases.

$\left(f_p/\sqrt{\varepsilon_h} = 12.1\ \text{GHz}\right)$. The spurious resonances appear due to the fact that in the close vicinity of the plasma frequency $\varepsilon_{zz} \to 0$, which, according to (17), invalidates our assumption on an electrically thin substrate. The issue of spurious resonances has been discussed in more detail in [28]. The results of Fig. 2 suggest that, for the considered geometry, the effects of spatial dispersion are negligible. It should be emphasized that this characteristic is radically different from the results obtained for a grounded wire medium slab with no patch array, for which, as demonstrated in [25], the wire medium slab has a completely different electromagnetic response.

Outside of the very narrow frequency band of the spurious resonances, both models also show an additional physical resonance for oblique incidence. This resonance occurs due to epsilon-near zero value of ε_{zz}.

To further understand the physical reasons why the effects of spatial dispersion are negligible for this example, we have plotted in Fig. 3(a) the magnitude of the normalized current profile along the vias. It can be seen that the current varies very little along the wires. The phase of the current (not reported here for brevity) is also practically constant. This behavior of the electric current is consistent with the hypotheses used to derive the ENG model, and in particular, imply that the electromagnetic fields below the patch grid are nearly uniform along z, i.e., $\partial/\partial z \approx 0$. Thus, in the spectral (Fourier) domain, the electromagnetic field amplitude in the wire medium has a peak at $q_z \approx 0$. This explains the suppression of spatial dispersion because the nonlocal dielectric function (4) is coincident with the local dielectric function (15) when $q_z = 0$.

In Fig. 4, the reflection phase obtained with the SD and ENG models for the second example are compared against the simulation results. The models are in a good agreement with each other below 20 GHz. The disagreement between the models becomes more noticeable as the frequency increases. The HFSS simulation results are in a very good agreement with the results of the SD model through the entire frequency band. If we look at the normalized current magnitudes plotted in Fig. 3(b) for the incidence angle of 30° at 10 GHz, we see that the current magnitude changes somewhat. In this case, the current phase remains constant. However, at 25 GHz (the slab is electrically thicker), the current magnitude changes drastically and the current phase is no longer constant. This causes the charges to accumulate on the wires and the effects of spatial dispersion are no longer negligible.

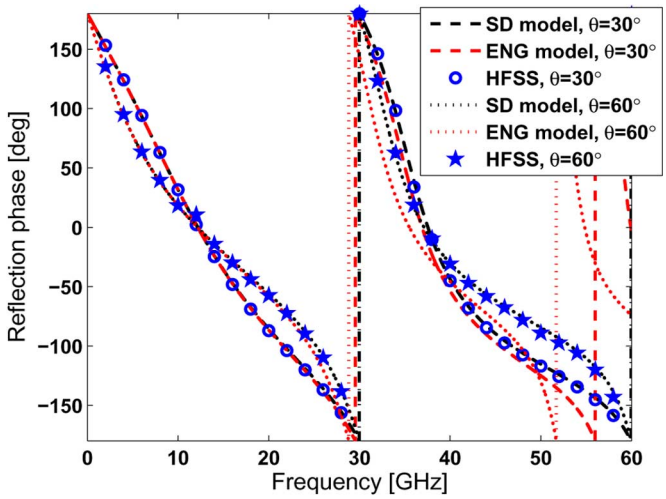

Fig. 4. Reflection phase calculated using the SD model in (12) and the ENG model in (16) for the second example: $a = 1$ mm, $g = 0.1$ mm, $h = 5$ mm, $\varepsilon_r = 1$, and $r_0 = 0.05$ mm.

The results in Figs. 2 and 4 suggest that the SD and ENG models give the same results when the current along the vias is essentially constant, or equivalently when the wire medium slab is electrically thin ($kh \ll 1$) and the height of the metallic pins is small as compared to the lattice constant $h/a < 1$. Indeed, it may be verified by a straightforward analysis that, under these assumptions, the normalized surface admittances in (18) and (19) reduce to

$$y_{s,\text{SD}} \approx \frac{\varepsilon_{zz}^{\text{TM}}}{\gamma_{\text{TM}}^2 h} + \frac{\varepsilon_{zz}^{\text{TM}} - \varepsilon_h}{k^2 h} = \frac{\varepsilon_h}{\gamma_{\text{loc}}^2 h} \tag{20}$$

$$y_{s,\text{ENG}} \approx \frac{\varepsilon_h}{\gamma_{\text{loc}}^2 h} \tag{21}$$

respectively. Here, we have used the fact that $k_p \sim 1/a$.

Besides the case where the current along the wires is nearly uniform, the effects of spatial dispersion may also be negligible in the regime where the wire medium is characterized by extreme anisotropy ($\varepsilon_{zz} \to -\infty$, $\varepsilon_{xx} = \varepsilon_{yy} = \varepsilon_h$). This situation is illustrated in Fig. 4, where, notwithstanding the current varying drastically along the wires, the agreement between the ENG and SD models is good. These results are explained by the fact that the wire medium is operated well below the plasma frequency. Indeed, if we assume $k_p \gg k$, we have, for the relative effective permittivity along the wires in the nonlocal model for the TM polarization, $\varepsilon_{zz}^{\text{TM}} \approx 0$, and in the local model for the extraordinary mode, $\left|\varepsilon_{zz}^{\text{loc}}\right| \to \infty \Rightarrow \gamma_{\text{loc}} = jk_0\sqrt{\varepsilon_h}$. Under these assumptions, the normalized admittances in (18) and (19) both reduce to

$$y_{s,\text{SD}} \approx y_{s,\text{ENG}} \approx -\frac{\varepsilon_h}{k}\cot(kh) \tag{22}$$

which, in fact, corresponds to the normalized admittance according to the TEM model [34]. The above result proves that the reflection properties predicted by the two analytical models are indeed the same under the regime of extreme anisotropy.

However, when these conditions (i.e., uniform current or extreme anisotropy) are not observed, the response of the mushroom structures may be dominated by nonlocal effects. To illus-

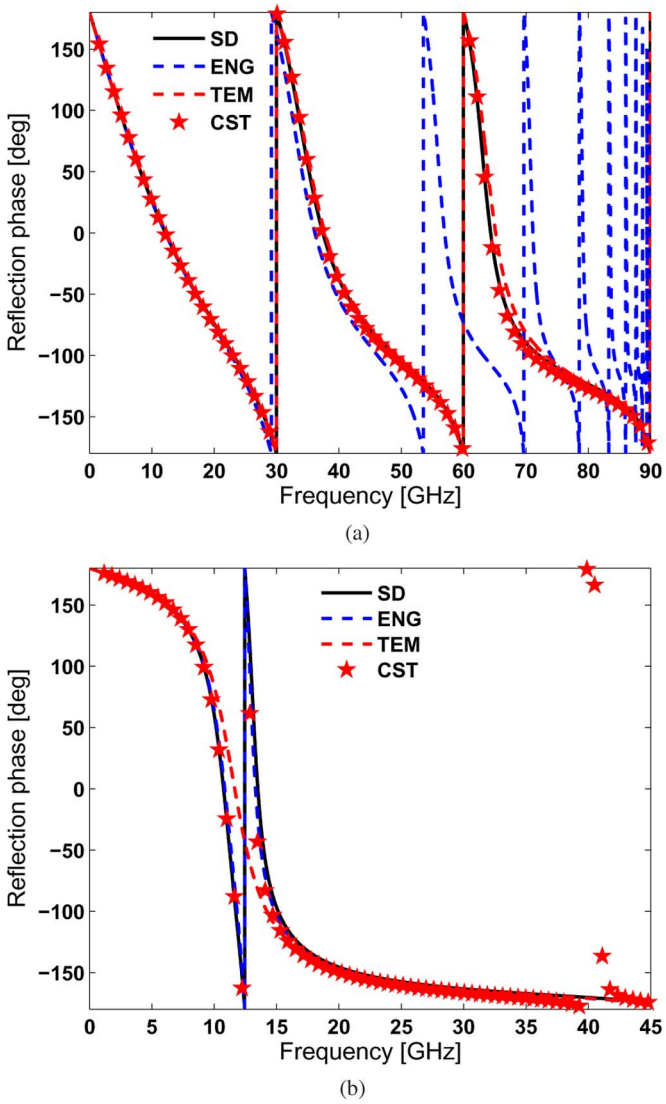

Fig. 5. Reflection phase for the: (a) second and (b) first example for the incidence angle of 45°. The reflection phases according to the SD, ENG, and TEM (see [34]) approximations (plotted with solid black, dashed blue (in online version), and red curves (in online version), respectively) are compared with each other and against CST-simulation results [plotted with red stars (in online version)]. The parameters for the structures are given in the text.

trate this, we plot in Fig. 5 the reflection phase calculated with the SD and ENG models for the same two examples considered before, and an angle of incidence of 45°. The star-shaped symbols in Fig. 5 correspond to full-wave results obtained with the commercial simulator CST Microwave Studio . As can be seen, in this example, where $h/a \gg 1$, the SD results are in very good agreement with full-wave simulations, whereas the ENG model only gives meaningful results for frequencies well below the plasma frequency, where, as discussed earlier, the material is characterized by extreme anisotropy and spatial dispersion is suppressed. Quite interestingly, in the regime where $h/a \gg 1$, the response of the structure is dominated by the effects of the TEM mode, consistent with the results of [24]. The TEM approximation corresponds to the case where the only mode excited in the wire medium is the TEM mode, i.e., the TM mode is discarded when calculating the response from the wire medium slab. According to the analysis in [34], when $h/a \gg 1$, the TM mode in the wire medium is nearly suppressed. To confirm this, we have plotted in Fig. 5 the results obtained under such TEM approximation. These results are obtained by considering that $A_{\mathrm{TM}} = 0$ in (8) and imposing only the boundary conditions (10) and (11) at the interface $z = 0$. The results of Fig. 5(a) (the plasma frequency, $f_p/\sqrt{\varepsilon_h} \approx 92.1$ GHz) show that, in fact, the TEM approximation agrees well with the SD model and with the simulation results, whereas the ENG model begins to disagree with the simulated results when the electrical thickness of the slab becomes comparable with the wavelength. However, the results in Fig. 5(b) for the first example of mushroom structure ($f_p/\sqrt{\varepsilon_h} \approx 12.1$ GHz)) show that, in the vicinity of the plasma frequency, the TEM model fails, as expected, whereas the SD and ENG models fit well with the CST simulations (until the limit $ka = \pi$, after which the homogenization fails). Indeed, the TEM approximation is suitable only for frequencies well below the plasma frequency.

IV. Discussion and Conclusions

In this paper, the reflection characteristics of mushroom-type high-impedance surface were studied. Two analytical models, namely, the ENG and SD models, were investigated for the electromagnetic response of high-impedance surfaces formed by a capacitive array over a grounded dielectric slab perforated with metallic pins. We derived the novel analytical (SD) model for the mushroom structure that takes the SD characteristics of the grounded wire medium slab into account. Using this and a simpler model from our previous work (ENG model), we studied the effect of the spatial dispersion in the wire medium on the reflection properties of the mushroom structure.

Surprisingly, our results demonstrate that the two models concur very well in a regime where the thickness of the slab is much smaller than the radiation wavelength, or alternatively, when the wire medium is characterized by extreme anisotropy ($\varepsilon_{zz} \to -\infty$, $\varepsilon_{xx} = \varepsilon_{yy} = \varepsilon_h$). In these conditions, the wire medium slab may, indeed, be regarded as a uniaxial material with negative permittivity. This property contrasts markedly with other wire medium topologies for which the effects of spatial dispersion are dominant [23], [25]. This dramatically different behavior is explained by the fact that when the wires are connected to the metallic patches/ground plane, the charges no longer accumulate at the tips of the metallic vias and do not create the additional current flow on the vias that would cause the SD effects. Hence, the current along the wires can be nearly uniform, and as a consequence, no matter what the incidence angle is, the ratio between the induced electric dipole moment and the surrounding macroscopic electric field component parallel to the wires remains the same. Due to this, a plasmonic resonance will occur at the same frequency for all incidence angles having an electric field component parallel to the wires.

Furthermore, the assumptions behind the ENG model are verified by the results of this paper. We validated the novel model using full-wave simulations, showing that it is very accurate even when the current amplitude and phase vary considerably. We also discussed the validity limits of the ENG model. It can be concluded that the spatial dispersion in the wire medium of the

mushroom-type high-impedance surface structure can be suppressed in particular designs, i.e., when the patch size is sufficiently large and the mushroom structure is electrically thin. This applies to most of the practical high-impedance surface structures.

REFERENCES

[1] P.-S. Kildal, "Artificially soft and hard surfaces in electromagnetics," *IEEE Trans. Antennas Propag.*, vol. 38, no. 10, pp. 1537–1544, Oct. 1990.

[2] D. Sievenpiper, L. Zhang, R. F. J. Broas, N. G. Alexopoulos, and E. Yablonovich, "High-impedance electromagnetic surfaces with a forbidden frequency band," *IEEE Trans. Microw. Theory Tech.*, vol. 47, no. 11, pp. 2059–2074, Nov. 1999.

[3] F.-R. Yang, K.-P. Ma, Y. Qian, and T. Itoh, "A novel TEM waveguide using uniplanar compact photonic-bandgap (UC-PBG) structure," *IEEE Trans. Microw. Theory Tech.*, vol. 47, no. 11, pp. 2092–2098, Nov. 1999.

[4] J. A. Higgins, H. Xin, A. Sailer, and M. Rosker, "Ka-band waveguide phase shifter using tunable electromagnetic crystal sidewalls," *IEEE Trans. Microw. Theory Tech.*, vol. 51, no. 4, pp. 1281–1287, Apr. 2003.

[5] O. Luukkonen, C. Simovski, A. V. Räisänen, and S. A. Tretyakov, "An efficient and simple analytical model for analysis of propagation properties in impedance waveguides," *IEEE Trans. Microw. Theory Tech.*, vol. 56, no. 7, pp. 1624–1632, Jul. 2008.

[6] F. Yang and Y. Rahmat-Samii, "Microstrip antennas integrated with electromagnetic band-gap (EBG) structures: A low mutual coupling design for array applications," *IEEE Trans. Antennas Propag.*, vol. 51, no. 10, pp. 2936–2946, Oct. 2003.

[7] A. P. Feresidis, G. Goussetis, S. Wang, and J. C. Vardaxoglou, "Artificial magnetic conductor surfaces and their application to low-profile high-gain planar antennas," *IEEE Trans. Antennas Propag.*, vol. 53, no. 1, pp. 209–215, Jan. 2005.

[8] J. M. Bell and M. F. Iskander, "A low-profile Archimedean spiral antenna using an EBG ground plane," *IEEE Antennas Wireless Propag. Lett.*, vol. 3, no. 1, pp. 223–226, 2004.

[9] D. Sievenpiper, J. Schaffner, J. J. Lee, and S. Livingston, "A steerable leaky-wave antenna using a tunable impedance ground plane," *IEEE Antennas Wireless Propag. Lett.*, vol. 1, no. 1, pp. 179–182, 2002.

[10] D. F. Sievenpiper, "Forward and backward leaky wave radiation with large effective aperture from an electronically tunable textured surface," *IEEE Trans. Antennas Propag.*, vol. 53, no. 1, pp. 236–247, Jan. 2005.

[11] N. Engheta, "Thin absorbing screens using metamaterial surfaces," in *IEEE AP-S Int. Symp. Dig.*, San Antonio, TX, 2002, vol. 2,, pp. 392–395.

[12] S. A. Tretyakov and S. I. Maslovski, "Thin absorbing structure for all incident angles based on the use of a high-impedance surface," *Microw. Opt. Technol. Lett.*, vol. 38, no. 3, pp. 175–178, 2003.

[13] Q. Gao, Y. Yin, D.-B. Yan, and N.-C. Yuan, "A novel radar-absorbing-material based on EBG structure," *Microw. Opt. Technol. Lett.*, vol. 47, no. 3, pp. 228–230, 2005.

[14] S. Simms and V. Fusco, "Thin absorber using artificial magnetic ground plane," *Electron. Lett.*, vol. 41, no. 24, pp. 1311–1313, 2005.

[15] S. Maci, M. Caiazzo, A. Cucini, and M. Casaletti, "A pole-zero matching method for EBG surfaces composed of a dipole FSS printed on a grounded dielectric slab," *IEEE Trans. Antennas Propag.*, vol. 53, no. 1, pp. 70–81, Jan. 2005.

[16] G. Goussettis, A. P. Feresidis, and J. C. Vardaxoglou, "Tailoring the AMC and EBG characteristics of periodic metallic arrays printed on grounded dielectric substrate," *IEEE Trans. Antennas Propag.*, vol. 54, no. 1, pp. 82–89, Jan. 2006.

[17] S. Clavijo, R. E. Díaz, and W. E. McKinzie, III, "High-impedance surfaces: An artificial magnetic conductor for a positive gain electrically small antennas," *IEEE Trans. Antennas Propag.*, vol. 51, no. 10, pp. 2678–2690, Oct. 2003.

[18] O. Luukkonen, C. Simovski, G. Granet, G. Goussetis, D. Lioubtchenko, A. V. Räisänen, and S. A. Tretyakov, "Simple and accurate analytical model of planar grids and high-impedance surfaces comprising metal strips or patches," *IEEE Trans. Antennas Propag.*, vol. 56, no. 6, pp. 1624–1632, Jun. 2008.

[19] J. Brown, "Artificial dielectrics," *Progr. Dielect.*, vol. 2, pp. 195–225, 1960.

[20] W. Rotman, "Plasma simulation by artificial dielectrics and parallel-plate media," *IRE Trans. Antennas Propag.*, vol. AP-10, no. 1, pp. 82–95, Jan. 1962.

[21] P. A. Belov, R. Marqués, S. I. Maslovski, I. S. Nefedov, M. Silveirinha, C. R. Simovski, and S. A. Tretyakov, "Strong spatial dispersion in wire media in the very large wavelength limit," *Phys. Rev. B, Condens. Matter*, vol. 67, 2003, Art. ID 113103.

[22] P. Belov, C. Simovski, and P. Ikonen, "Canalization of subwavelength images by electromagnetic crystals," *Phys. Rev. B, Condens. Matter*, vol. 71, 2005, Art. ID 193105.

[23] P. Belov, Y. Hao, and S. Sudhakaran, "Subwavelength microwave imaging using an array of parallel conducting wires as a lens," *Phys. Rev. B, Condens. Matter*, vol. 73, 2006, Art. ID 033108.

[24] P. Ikonen, P. Belov, C. Simovski, Y. Hao, and S. Tretyakov, "Magnification of subwavelength field distributions at microwave frequencies using a wire medium slab operating in the canalization regime," *Appl. Phys. Lett.*, vol. 91, 2007, Art. ID 104102.

[25] M. G. Silveirinha, C. A. Fernandes, and J. R. Costa, "Electromagnetic characterization of textures surfaces formed by metallic pins," *IEEE Trans. Antennas Propag.*, vol. 56, no. 2, pp. 405–415, Feb. 2008.

[26] M. G. Silveirinha, C. A. Fernandes, and J. R. Costa, "Additional boundary condition for a wire medium connected to a metallic surface," *New J. Phys.*, vol. 10, 2008, Art. ID 053011.

[27] M. Silveirinha, "Additional boundary condition for the wire medium," *IEEE Trans. Antennas Propag.*, vol. 54, no. 6, pp. 1766–1766, Jun. 2006.

[28] O. Luukkonen, F. Costa, A. Monorchio, and S. A. Tretyakov, "A thin electromagnetic absorber for wide incidence angles and both polarizations," 2009. [Online]. Available: http://arxiv.org/abs/0807.4831v3

[29] A. B. Yakovlev, C. R. Simovski, S. A. Tretyakov, O. Luukkonen, G. W. Hanson, S. Paulotto, and P. Baccarelli, "Analytical modeling of surface waves on high impedance surfaces," in *Proc. NATO Adv. Res. Workshop*, Marrakesh, Morocco, May 2008, pp. 184–193.

[30] O. Luukkonen, M. G. Silveirinha, A. B. Yakovlev, C. R. Simovski, I. S. Nefedov, and S. A. Tretyakov, "Homogenization models for the analysis of reflection properties of mushroom structures," in *Proc. 2nd Int. Adv. Electromagn. Mater. Microw. Opt. Congr.*, Pamplona, Spain, Sep. 21–26, 2008, pp. 208–210.

[31] A. B. Yakovlev, M. G. Silveirinha, O. Luukkonen, C. R. Simovski, I. S. Nefedov, and S. A. Tretyakov, "Homogenization models for the analysis of surface waves on analysis of surface waves on mushroom structures," in *Proc. 2nd Int. Adv. Electromagn. Mater. Microw. Opt. Congr.*, Pamplona, Spain, Sep. 21–26, 2008, pp. 310–312.

[32] A. B. Yakovlev, O. Luukkonen, C. R. Simovski, S. A. Tretyakov, S. Paulotto, P. Baccarelli, and G. W. Hanson, "Analytical modeling of surface waves on high impedance surfaces," in *Metamaterials and Plasmonics: Fundamentals, Modelling, Applications*, ser. NATO Sci. for Peace and Security B, S. Zouhdi, A. Sihvola, and A. P. Vinogradov, Eds. Dordrecht,, The Netherlands: NATO, 2009, pp. 239–254.

[33] A. Demetriadou and J. Pendry, "Taming spatial dispersion in wire metamaterial," *J. Phys., Condens. Matter*, vol. 20, 2008, Art. ID 295222.

[34] S. A. Tretyakov, *Analytical Modeling in Applied Electromagnetics*. Norwood, MA: Artech House, 2003, pp. 231–231.

Olli Luukkonen received the M.Sc. degree in electrical engineering from the TKK Helsinki University of Technology, Espoo, Finland, in 2006, and is currently working toward the Ph.D. degree at the TKK Helsinki University of Technology.

He is currently a Research Engineer with the Department of Radio Science and Engineering, TKK Helsinki University of Technology. His current research interests include artificial electromagnetic materials, surfaces, and their applications.

Mário G. Silveirinha (S'99–M'03) received the Licenciado degree in electrical engineering from the Universidade de Coimbra, Coimbra, Portugal, in 1998, and the Ph.D. degree in electrical and computer engineering from the Instituto Superior Técnico (IST), Technical University of Lisbon, Lisbon, Portugal, in 2003.

Since 2003, he has been an Assistant Professor with the Universidade de Coimbra. His research interests include electromagnetic wave propagation in structured materials and homogenization theory.

Alexander B. Yakovlev (S'94–M'97–SM'01) received the Ph.D. degree in radiophysics from the Institute of Radiophysics and Electronics, National Academy of Sciences, Kharkov, Ukraine, in 1992, and the Ph.D. degree in electrical engineering from the University of Wisconsin at Milwaukee, in 1997.

In 2000, he joined the Department of Electrical Engineering, The University of Mississippi, as an Assistant Professor, and became an Associate Professor in 2004. He coauthored *Operator Theory for Electromagnetics: An Introduction* (Springer, 2002). From 2003 to 2006, he was an Associate Editor-in-Chief of the ACES Journal. His research interests include mathematical methods in applied electromagnetics, homogenization models for metamaterials, artificial impedance surfaces, and EBG structures, theory of leaky waves, and catastrophe and bifurcation theories.

Dr. Yakovlev is a member of URSI Commission B. From 2005 to 2008, he was an associate editor of the IEEE TRANSACTIONS ON MICROWAVE THEORY AND TECHNIQUES. He was the recipient of the Young Scientist Award presented at the 1992 URSI International Symposium on Electromagnetic Theory, Sydney, Australia, and the Young Scientist Award presented at the 1996 International Symposium on Antennas and Propagation, Chiba, Japan.

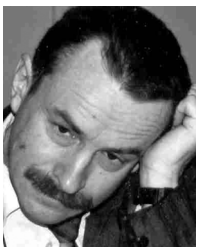

Constantin R. Simovski (M'92) was born in Leningrad, Russian Republic of Soviet Union (now St. Petersburg), Russia, on December 7, 1957. He received the Diploma of Engineer Researcher degree in radio engineering, the Ph.D. degree in electromagnetic theory, and Doctor of Sciences degree from the St. Petersburg State Polytechnic University (formerly the Leningrad Polytechnic Institute and State Technical University), St. Petersburg, Russia, in 1980, 1986, and 2000, respectively. In 1986, he defended the thesis of a Candidate of Science (Ph.D.) (a study of the scattering of Earth waves in the mountains) at the Leningrad Polytechnic Institute. In 2000, he defended the thesis of Doctor of Sciences (a theory of 2-D and 3-D bianisotropic scattering arrays).

From 1980 to 1992, he was with the Soviet scientific and industrial firm Impulse. In 1992, he joined the St. Petersburg University of Information Technologies, Mechanics and Optics, as an Assistant, where from 1994 to 1995, he was an Assistant Professor, from 1995 to 2001, he was an Associate Professor, and since 2001, he has been a Full Professor. Since 1999, he has been involved in the theory and applications of 2-D and 3-D EBG structures for microwave and ultrashort-wave antennas. He is currently with the TKK Helsinki University of Technology, Espoo, Finland, where his research concerns the field of metamaterials for microwave and optical applications including optics of metal nanoparticles.

Igor S. Nefedov (M'92) received the Dipl. Physicist, Candidate of Sciences (Ph.D.), and Doctor of Sciences degrees in radio-physics from Saratov State University (SSU), Saratov, Russia, in 1972, 1981, and 1998, respectively.

From 1975 to 1992, he was with the Research Institute of Mechanics and Physics, SSU. Since 1992, he has been with the Institute of Radio Engineering and Electronics, Russian Academy of Science, Saratov, Russia. He has been a Visiting Professor with the Radio Laboratory, TKK Helsinki University of Technology (20012002) and Full Professor with SSU (20032004). He has been a Visiting Researcher in Italy, Germany, Poland, France and Belgium. Since 2004, he has been a Senior Researcher with the TKK Helsinki University of Technology. His main scientific interests are electromagnetic field theory, electromagnetics of complex media, and optics.

Sergei A. Tretyakov (M'92–SM'98–F'08) received the Dipl. Engineer-Physicist, Candidate of Sciences (Ph.D.), and Doctor of Sciences degrees in radiophysics from the St. Petersburg State Technical University, St. Petersburg, Russia, in 1980, 1987, and 1995, respectively.

From 1980 to 2000, he was with the Radiophysics Department, St. Petersburg State Technical University. He is currently a Professor of radio engineering with the Department of Radio Science and Engineering, TKK Helsinki University of Technology, Espoo, Finland, and President of the Metamorphose Virtual Institute. His main scientific interests are electromagnetic field theory, complex media electromagnetic, and microwave engineering.

Prof. Tretyakov was chairman of the St. Petersburg IEEE Electron Devies (ED)/Microwave Theory and Techniques (MTT)/Antennas and Propagation (AP) Chapter from 1995 to 1998.